



## OPEN ACCESS

## EDITED BY

Francesca Innocenti,  
Careggi University Hospital, Italy

## REVIEWED BY

Constantina Aggeli,  
National and Kapodistrian University of Athens,  
Greece

Antoine AbdelMassih,  
Cairo University, Egypt

## \*CORRESPONDENCE

Attila Nemes

✉ nemes.attila@med.u-szeged.hu

RECEIVED 09 January 2023

ACCEPTED 07 August 2023

PUBLISHED 04 September 2023

## CITATION

Nemes A, Kormányos Á, Rácz G, Ruzsa Z,  
Achim A, Ambrus N and Lengyel C (2023)  
Tricuspid annular and right atrial volume  
changes are associated in healthy adults—  
insights from the three-dimensional speckle-  
tracking echocardiographic MAGYAR-Healthy  
Study.

Front. Cardiovasc. Med. 10:1140599.

doi: 10.3389/fcvm.2023.1140599

## COPYRIGHT

© 2023 Nemes, Kormányos, Rácz, Ruzsa,  
Achim, Ambrus and Lengyel. This is an open-  
access article distributed under the terms of the  
[Creative Commons Attribution License \(CC BY\)](https://creativecommons.org/licenses/by/4.0/).  
The use, distribution or reproduction in other  
forums is permitted, provided the original  
author(s) and the copyright owner(s) are  
credited and that the original publication in this  
journal is cited, in accordance with accepted  
academic practice. No use, distribution or  
reproduction is permitted which does not  
comply with these terms.

# Tricuspid annular and right atrial volume changes are associated in healthy adults—insights from the three-dimensional speckle-tracking echocardiographic MAGYAR-Healthy Study

Attila Nemes\*, Árpád Kormányos, Gergely Rácz, Zoltán Ruzsa,  
Alexandru Achim, Nóra Ambrus and Csaba Lengyel

Department of Medicine, Albert Szent-Györgyi Medical School, University of Szeged, Szeged, Hungary

**Introduction:** The tricuspid valve and its annulus (TA) and the right atrium (RA) play a significant role in regulating blood flow in the right heart. However, their effect on each other is not fully understood even in normal circumstances. Three-dimensional (3D) speckle-tracking echocardiography (3DSTE) is able to simultaneously assess TA and RA at the same time in a non-invasive way. The present study aimed to examine associations between tricuspid annular (TA) dimensions and right atrial (RA) volumes in healthy adults by 3DSTE.

**Methods:** The present study comprised 144 healthy subjects (mean age:  $34.4 \pm 12.6$  years, 72 males), who participated in this study on a voluntary basis for screening between 2011 and 2015. In all subjects, electrocardiography, two-dimensional Doppler echocardiography and 3DSTE have been performed.

**Results:** With increasing end-systolic maximum RA volume, all end-systolic and end-diastolic TA dimensions showed simultaneous increase, but in various degrees resulting in (non-significant) reduction of TA functional properties. Similarly, with increasing diastolic pre-atrial contraction and minimum RA volumes, TA dimensions increased simultaneously (except end-diastolic TA diameter), but in various degrees resulting in reduced TA fractional shortening and fractional area change. With increasing RA dimensions, end-systolic and end-diastolic TA dimensions showed simultaneous increase, but in different, sometimes not significant degrees. While RA stroke volumes showed increasing pattern with TA dilation, RA emptying fractions have not changed substantially.

**Conclusions:** 3DSTE is suitable for non-invasive assessment of TA dimensions and RA volumes at the same time using the same 3D echocardiographic dataset. Significant associations between TA size and RA volumes exist in healthy circumstances. Strong associations in case of dilation of TA in the presence of higher RA volumes could partly explain functional tricuspid regurgitation later developing in subjects in sinus rhythm.

## KEYWORDS

healthy, tricuspid annulus, right atrial, volume, three-dimensional, speckle-tracking, echocardiography

## Introduction

In recent years, there has been an increasing interest in the evaluation of the right heart due to newer therapeutic options and advanced imaging techniques (1–4). New findings help to better understand the right heart, its components, their characteristics and interactions, even with the aorta, left heart and venous system, and their dependence on each other (1–4). The tricuspid valve (TV) and its annulus (TA) and the right atrium (RA) play a significant role in regulating blood flow in the right heart. Their effect on each other was examined in subjects with functional tricuspid regurgitation (FTR) (5–7) and even in healthy normal circumstances (8, 9). Three-dimensional speckle-tracking echocardiography (3DSTE) is able to simultaneously assess TA and RA in detail at the same time in a non-invasive way (10–12). The present study aimed to examine associations between tricuspid annular (TA) dimensions and right atrial (RA) volumes respecting the cardiac cycle in healthy adults by 3DSTE.

## Patients and methods

### Study population

The present study comprised 144 healthy subjects (mean age:  $34.4 \pm 12.6$  years, 72 males), who participated in this study on a voluntary basis for screening between 2011 and 2015. In all subjects, electrocardiography (ECG), two-dimensional Doppler echocardiography (2DE) and 3DSTE have been performed by the same observer (ÁK). A participant was considered to be healthy if they had no acute or chronic illness in their medical history, ECG showed no abnormality, and findings of complete 2DE were in normal ranges. None of the subjects were obese, smoker or had a history of regular drug use. The present study is part of the Motion Analysis of the heart and Great vessels bY three-dimensional speckle-tRacking echocardiography in Healthy subjects (MAGYAR-Healthy) Study. This study aimed to evaluate the physiological associations among 3DSTE-derived and other parameters in healthy adults (“Magyar” means “Hungarian” in Hungarian language). The study was conducted in accordance with the Declaration of Helsinki (as revised in 2013). The study was approved by the Institutional and Regional Human Biomedical Research Committee of University of Szeged, Hungary (No.: 71/2011 and updated versions) and informed consent was given by all subjects.

### Two-dimensional Doppler echocardiography

In all cases, the same Toshiba Artida™ echocardiography equipment (Toshiba Medical Systems, Tokyo, Japan) was used

attached to a 1–5 MHz PST-30BT phased-array transducer. During chamber quantifications the rules prescribed in recent guidelines were followed (1). For visual quantification of valvular regurgitations and to exclude significant valvular stenosis, Doppler echocardiography was used. Early and late mitral inflow E and A were also determined to assess LV diastolic function (1, 13).

### Three-dimensional speckle-tracking echocardiography

The same Toshiba Artida™ echocardiographic equipment (Toshiba Medical Systems, Tokyo, Japan) was used for 3DSTE as well, but transducer was changed to a PST-25SX matrix-array transducer with 3DSTE capability (10–12, 14, 15). The protocol of the 3DSTE examination followed our routines: firstly, 3D echocardiographic datasets were acquired from the apical window following optimisation of image quality on the right atrium (RA). If RR intervals were constant on ECG (sinus rhythm) and subjects were on breath-hold, pyramid-shaped 3D echocardiographic datasets were digitally stored on hard drive for future analysis.

### RA-quantification by 3DSTE

Later, offline analysis was performed with the vendor-provided 3D Wall Motion Tracking software version 2.7 (Ultra Extend, Toshiba Medical Systems, Tokyo, Japan). Data were displayed in selected apical two- (AP2CH) and four-chamber (AP4CH) views and 3 short-axis views at basal, midatrial and superior levels. To create a 3D cast of the RA, definition of reference points on RA endocardium were required in AP2CH and AP4CH views on the edges of the TA ring and the RA apex at end-diastole, then automatic sequential analysis (reconstruction) was performed for the complete endocardial RA surface. Taking into account the cardiac cycle, the following RA volumes were obtained (Figure 1) (14):

- Maximum RA volume, measured at end-systole, just before tricuspid valve opening ( $V_{max}$ ).
- RA volume before atrial contraction, measured at early-diastole at the time of the P wave on the ECG ( $V_{preA}$ ).
- Minimum RA volume measured at end-diastole, just before tricuspid valve closure ( $V_{min}$ ).

Using RA volumes, several stroke volumes (SV) and emptying fractions (EF) could be determined featuring different phases of RA function:

*Reservoir function:*

- Total Atrial Stroke Volume (TASV):  $V_{max} - V_{min}$ .
- Total Atrial Emptying Fraction (TAEF):  $TASV / V_{max} \times 100$ .

*Conduit function:*

- Passive Atrial Stroke Volume (PASV):  $V_{max} - V_{preA}$ .
- Passive Atrial Emptying Fraction (PAEF):  $PASV / V_{max} \times 100$ .

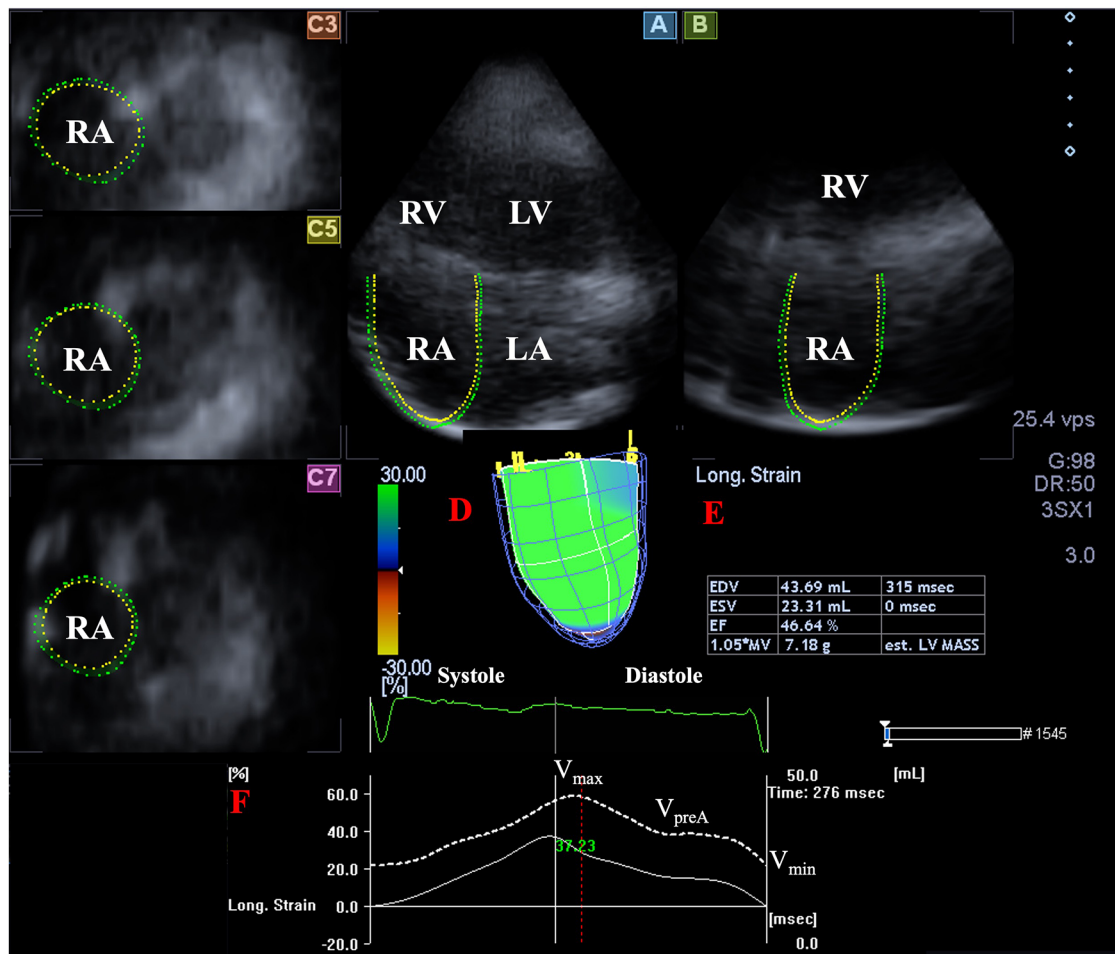


FIGURE 1

Three-dimensional (3D) speckle-tracking echocardiographic analysis of the right atrium in a healthy subject: apical longitudinal four-chamber (A) and two-chamber views (B) and 3 short-axis views at basal (C3), midatrial (C5) and superior (C7) RA levels. 3D virtual RA model (D), RA volumetric data (E) and time-global RA volume change curve (dashed white curve) and time-global RA longitudinal strain curve (white curve) respecting the cardiac cycle are demonstrated (F). LA, left atrium; LV, left ventricle; RA, right atrium; RV, right ventricle; EDV, end-diastolic volume; ESV, end-systolic volume; EF, ejection fraction; est., estimated; MV, myocardial volume;  $V_{max}$ , maximum right atrial volume;  $V_{preA}$ , volume at the onset of atrial systole;  $V_{min}$ , minimum right atrial volume.

#### Active contraction:

- Active Atrial Stroke Volume (AASV):  $V_{preA} - V_{min}$ .
- Active Atrial Emptying Fraction (AAEF):  $AASV / V_{preA} \times 100$ .

### TA-quantification by 3DSTE

During assessments, AP2CH and AP4CH views helped to find optimal lateral and septal TA endpoints on C7 short-axis view (Figure 2) (15):

Morphological parameters were measured at end-diastole (just before tricuspid valve closure) and at end-systole (just before tricuspid valve opening):

- TA diameter (TAD), measured by drawing a perpendicular line from the peak of TA curvature to the middle of the straight TA border,
- TA area (TAA), measured by planimetry,
- TA perimeter (TAP), measured by planimetry,

Functional parameters were calculated from morphologic end-diastolic and end-systolic parameters:

- TA fractional shortening (TAFS), defined as  $[(\text{end-diastolic TAD} - \text{end-systolic TAD}) / \text{end-diastolic TAD}] \times 100$ ,
- TA fractional area change (TAFAC), defined as  $[(\text{end-diastolic TAA} - \text{end-systolic TAA}) / \text{end-diastolic TAA}] \times 100$ .

### Statistical analysis

Data were presented in mean  $\pm$  standard deviation (SD) format or frequency/percentage format, as appropriate.  $p < 0.05$  was considered to be statistically significant. Student  $t$  test with Welch correction and one-way analysis of variance (ANOVA) test with Bonferroni correction were used, where appropriated. Fischer's exact test was used for all categorical variables. Pearson's correlation coefficient was calculated for correlations. The Bland-Altman method was used to determine intraobserver

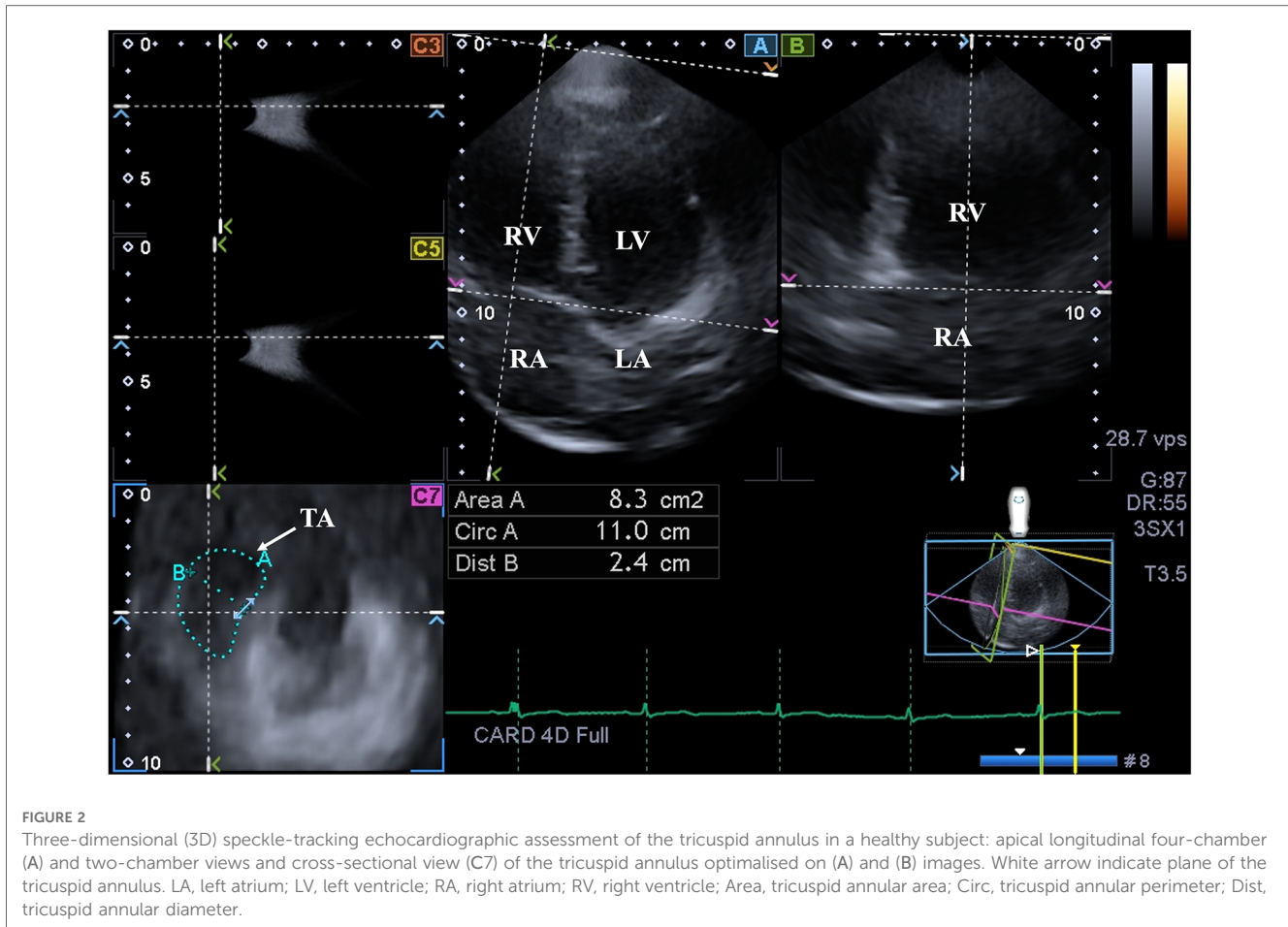


FIGURE 2

Three-dimensional (3D) speckle-tracking echocardiographic assessment of the tricuspid annulus in a healthy subject: apical longitudinal four-chamber (A) and two-chamber views and cross-sectional view (C7) of the tricuspid annulus optimised on (A) and (B) images. White arrow indicate plane of the tricuspid annulus. LA, left atrium; LV, left ventricle; RA, right atrium; RV, right ventricle; Area, tricuspid annular area; Circ, tricuspid annular perimeter; Dist, tricuspid annular diameter.

and interobserver agreements. For intraobserver and interobserver correlations, intraclass correlation coefficients (ICCs) were calculated. Multivariable regression analysis was used for assessment of independent predictors of  $V_{max}$  and TAA-D. GPower 3.1.9 Software (Heinrich-Heine Universität, Düsseldorf, Germany) was applied for power calculation: in the presence of effect size: 0.9, alpha: 0.05, power: 0.8 the minimum group size is  $n = 120$ . Statistical calculations were performed using SPSS software (SPSS Inc, Chicago, IL, USA).

## Results

### Clinical and two-dimensional Doppler echocardiographic data

Clinical and routine echocardiographic parameters of healthy adults are presented in **Table 1**. None of the subjects involved had larger than or equal to grade 1 valvular regurgitation or showed significant valvular stenosis on any valves.

### Classification of subjects

Mean  $\pm$  SD of 3DSTE-derived RA and TA parameters of healthy subjects are presented in **Table 2**. Healthy subjects were

classified into 3 groups according to the normal maximum ( $V_{max}$ ), pre-atrial contraction ( $V_{preA}$ ) and minimum ( $V_{min}$ ) RA volumes and end-systolic and end-diastolic TA diameter (TAD-S and TAD-D, respectively), area (TAA-S and TAA-D, respectively) and perimeter (TAP-S and TAP-D, respectively): estimated mean  $\pm$  SD served as the lower (33.8 ml, 24.8 ml, 18.1 ml, 1.5 cm, 2.1 cm, 4.0 cm<sup>2</sup>, 5.7 cm<sup>2</sup>, 7.9 cm, 9.3 cm, respectively) and upper (64.0 ml, 46.8 ml, 37.5 ml, 2.1 cm, 2.7 cm, 6.8 cm<sup>2</sup>, 8.9 cm<sup>2</sup>, 10.1 cm, 11.7 cm, respectively) values.

### Increase of RA volumes and TA

With increasing end-systolic  $V_{max}$ , all end-systolic and end-diastolic TA dimensions showed simultaneous increase, but in various degrees resulting in (non-significant) reduction of TA functional properties. Similarly, with increasing diastolic  $V_{preA}$  and  $V_{min}$ , TA dimensions increased simultaneously (except TAD-D), but in various degrees resulting in reduced TAFS and TAFAC (**Table 3**).

### Increase of RA volumes and RA volume-based functional properties

With increasing end-systolic  $V_{max}$ , all SVs and EFs showed simultaneous increase, except AAEF, which remained unchanged.

TABLE 1 Clinical and two-dimensional echocardiographic data.

Data	Measures
<b>Clinical data</b>	
<i>n</i>	144
Mean age (years)	34.4 ± 12.6
Males (%)	72 (50%)
Systolic blood pressure (mmHg)	121.4 ± 4.1
Diastolic blood pressure (mmHg)	78.9 ± 3.4
Heart rate (1/s)	71.3 ± 2.1
Height (cm)	170.8 ± 10.3
Weight (kg)	72.9 ± 15.5
Body surface area (kg/m <sup>2</sup> )	1.87 ± 0.36
<b>Two-dimensional echocardiographic data</b>	
LA diameter (mm)	37.8 ± 3.1
LV end-diastolic diameter (mm)	48.4 ± 3.1
LV end-systolic diameter (mm)	32.5 ± 2.6
LV end-diastolic volume (ml)	106.3 ± 23.3
LV end-systolic volume (ml)	38.2 ± 8.9
Interventricular septum (mm)	9.3 ± 1.1
LV posterior wall (mm)	9.4 ± 1.2
LV ejection fraction (%)	65.1 ± 3.5
Early diastolic mitral inflow velocity—E (cm/s)	79.4 ± 16.5
Late diastolic mitral inflow velocity—A (cm/s)	60.0 ± 15.0

LA, left atrial; LV, left ventricular.

TABLE 2 Three-dimensional speckle-tracking echocardiography-derived right atrial volumetric and tricuspid annular parameters.

Parameters	Measures
Maximum right atrial volume ( $V_{\max}$ , ml)	48.9 ± 15.1
Pre-atrial contraction left atrial volume ( $V_{\text{preA}}$ , ml)	35.8 ± 11.0
Minimum left atrial volume ( $V_{\min}$ , ml)	27.8 ± 9.7
Total atrial stroke volume (TASV, ml)	21.1 ± 10.0
Total atrial emptying fraction (TAEF, %)	42.5 ± 12.6
Passive atrial stroke volume (PASV, ml)	13.1 ± 8.3
Passive atrial emptying fraction (PAEF, %)	25.8 ± 11.7
Active atrial stroke volume (AASV, ml)	8.0 ± 4.8
Active atrial emptying fraction (AAEF, %)	22.5 ± 11.6
End-systolic tricuspid annular diameter (TAD-S, mm)	1.8 ± 0.3
End-systolic tricuspid annular area (TAA-S, mm <sup>2</sup> )	5.4 ± 1.4
End-systolic tricuspid annular perimeter (TAP-S, mm)	9.0 ± 1.1
End-diastolic tricuspid annular diameter (TAD-D, mm)	2.4 ± 0.3
End-diastolic tricuspid annular area (TAA-D, mm <sup>2</sup> )	7.3 ± 1.6
End-diastolic tricuspid annular perimeter (TAP-D, mm)	10.5 ± 1.2
Tricuspid annular fractional shortening (TAFS, %)	21.4 ± 8.8
Tricuspid annular fractional area change (TAFAC, %)	26.4 ± 10.6

With increasing diastolic  $V_{\text{preA}}$ , while SVs showed increasing pattern, EFs had decreasing pattern. With increasing diastolic  $V_{\min}$ , while SVs remained unchanged, EFs showed decreasing pattern (Table 3).

## Dilation of TA and RA volumes

With increasing TA dimensions, end-systolic and end-diastolic RA dimensions showed simultaneous increase, but in different degrees. While SVs showed increasing pattern with TA dilation, EFs have not changed substantially (Tables 4, 5).

## Dilation of TA and TA functional properties

With increasing end-systolic TA dimensions, TA functional properties showed simultaneous decrease, but in different degrees. With increasing end-diastolic TAD-D, TAFS increased, TAFAC remained unchanged. With increasing end-diastolic TAA-D and TAP-D, TA functional properties did not show significant changes (Tables 4, 5).

## Correlations and regression analysis

$V_{\max}$  correlated with TAD-D ( $r = 0.30$ ,  $p < 0.01$ ), TAA-D ( $r = 0.54$ ,  $p < 0.01$ ), TAA-P ( $r = 0.50$ ,  $p < 0.01$ ), TAD-S ( $r = 0.39$ ,  $p < 0.01$ ), TAA-S ( $r = 0.55$ ,  $p < 0.01$ ) and TAA-P ( $r = 0.49$ ,  $p < 0.01$ ). Similarly,  $V_{\text{preA}}$  showed correlations with TAD-D ( $r = 0.25$ ,  $p < 0.01$ ), TAA-D ( $r = 0.49$ ,  $p < 0.01$ ), TAA-P ( $r = 0.45$ ,  $p < 0.01$ ), TAD-S ( $r = 0.40$ ,  $p < 0.01$ ), TAA-S ( $r = 0.58$ ,  $p < 0.01$ ) and TAA-P ( $r = 0.49$ ,  $p < 0.01$ ).  $V_{\min}$  correlated with TAD-D ( $r = 0.54$ ,  $p < 0.01$ ), TAA-D ( $r = 0.48$ ,  $p < 0.01$ ), TAA-P ( $r = 0.41$ ,  $p < 0.01$ ), TAD-S ( $r = 0.37$ ,  $p < 0.01$ ), TAA-S ( $r = 0.54$ ,  $p < 0.01$ ) and TAA-P ( $r = 0.46$ ,  $p < 0.01$ ), as well.

The logistic regression analysis identified presence of increased  $V_{\max}$  as an independent predictor of TAA-D [hazard ratio (HR) 1.75, 95% CI of HR: 1.18 to 3.33,  $p < 0.05$ ]. Similarly, dilated TAA-D had an independent predictive value for  $V_{\max}$  [hazard ratio (HR) 1.80, 95% CI of HR: 1.15 to 3.27,  $p < 0.05$ ].

## Feasibility of 3DSTE-derived RA and TA measurements

During evaluations, 94 subjects were excluded due to inferior image quality from the total of 238 subjects, therefore the overall feasibility of simultaneous 3DSTE-derived RA and TA quantifications was 144 out of 238 (61% overall feasibility).

## Reproducibility of 3DSTE-derived RA and TA assessments

3DSTE-derived end-diastolic and end-systolic TA dimensions and RA volumes respecting cardiac cycle were measured twice by the same observer (intraobserver agreement) and by two independent observers (interobserver agreement). The values were expressed as mean ± SD together with corresponding ICCs, the results are presented in Table 6.

## Discussion

Components of the TV or right atrioventricular valve include fibrous TA, anterior, posterior and septal leaflets, papillary muscles and tendinous cords, which interact with RA and RV during the cardiac cycle. When TV opens in diastole, it helps correct one-way blood flow from the RA to the RV, while in

TABLE 3 Right atrial volumes and tricuspid annular parameters in different right atrial volume groups.

	$V_{max} \leq 33.8 \text{ ml}$ (n = 26)	$33.8 \text{ ml} < V_{max} < 64.0 \text{ ml}$ (n = 92)	$64.0 \text{ ml} \leq V_{max}$ (n = 26)	$V_{preA} \leq 24.8 \text{ ml}$ (n = 23)	$24.8 \text{ ml} < V_{preA} < 46.8 \text{ ml}$ (n = 100)	$46.8 \text{ ml} \leq V_{preA}$ (n = 21)	$V_{min} \leq 18.1 \text{ ml}$ (n = 22)	$18.1 \text{ ml} < V_{min} < 37.5 \text{ ml}$ (n = 93)	$37.5 \text{ ml} \leq V_{min}$ (n = 29)
$V_{max}$ (ml)	29.6 ± 3.4	47.5 ± 7.5*	73.7 ± 9.1***	31.7 ± 7.9	48.6 ± 10.7†	70.9 ± 13.3†,††	34.4 ± 9.7	47.1 ± 11.3‡	65.6 ± 14.6‡,‡‡
$V_{preA}$ (ml)	23.1 ± 4.1	35.1 ± 6.5*	50.5 ± 10.8***	21.4 ± 3.3	35.3 ± 5.5†	55.4 ± 8.4†,††	23.4 ± 6.2	33.9 ± 5.9‡	51.2 ± 9.7‡,‡‡
$V_{min}$ (ml)	18.1 ± 3.7	27.0 ± 7.4*	39.8 ± 8.1***	16.0 ± 2.9	27.1 ± 6.2†	44.8 ± 4.5†,††	15.3 ± 2.3	25.9 ± 4.7‡	43.3 ± 4.5‡,‡‡
TASV (ml)	11.5 ± 3.1	20.4 ± 7.7*	33.9 ± 8.9***	15.7 ± 8.0	21.4 ± 9.3†	26.1 ± 12.3†	19.1 ± 9.3	21.2 ± 9.2	22.3 ± 12.7
TAEF (%)	38.9 ± 9.4	42.8 ± 13.6	45.9 ± 10.1*	47.4 ± 12.4	42.9 ± 12.5	35.1 ± 10.7†,††	52.9 ± 12.1	43.4 ± 10.3‡	31.7 ± 12.0‡,‡‡
PASV (ml)	6.6 ± 3.4	12.3 ± 6.3*	23.2 ± 9.6***	10.4 ± 7.2	13.3 ± 7.9	15.5 ± 11.0	11.0 ± 7.7	13.2 ± 7.8	14.4 ± 10.3
PAEF (%)	22.1 ± 11.0	25.5 ± 11.2	31.4 ± 12.3***	30.4 ± 13.9	25.8 ± 10.9	20.4 ± 11.8†,††	30.0 ± 15.3	26.4 ± 10.4	20.5 ± 11.4‡,‡‡
AASV (ml)	4.9 ± 2.2	8.1 ± 4.6*	10.8 ± 5.6***	5.3 ± 2.5	8.1 ± 4.5†	10.6 ± 6.2†,††	8.1 ± 5.0	8.0 ± 3.9	8.0 ± 6.8
AAEF (%)	21.2 ± 8.8	23.4 ± 13.0	20.9 ± 8.4	24.6 ± 10.2	23.0 ± 12.3	18.2 ± 8.5†	32.2 ± 12.9	23.0 ± 9.4‡	13.9 ± 10.9‡,‡‡
TAD-S (mm)	1.7 ± 0.3	1.8 ± 0.2*	2.0 ± 0.4***	1.7 ± 0.3	1.8 ± 0.2†	2.0 ± 0.4†,††	1.7 ± 0.2	1.8 ± 0.2‡	1.9 ± 0.4‡
TAA-S (mm)	4.2 ± 1.2	5.4 ± 1.1*	6.6 ± 1.8***	4.4 ± 1.3	5.4 ± 1.2†	6.6 ± 1.9†,††	4.3 ± 1.3	5.4 ± 1.2‡	6.2 ± 1.8‡,‡‡
TAP-S (mm)	8.3 ± 1.2	9.0 ± 0.9*	9.9 ± 1.1***	8.5 ± 1.2	9.0 ± 1.0†	9.9 ± 1.2†,††	8.3 ± 1.2	9.0 ± 0.9‡	9.6 ± 1.2‡,‡‡
TAD-D (mm)	2.2 ± 0.3	2.3 ± 0.3*	2.5 ± 0.4***	2.3 ± 0.3	2.3 ± 0.3	2.5 ± 0.4	2.2 ± 0.4	2.4 ± 0.3	2.4 ± 0.4
TAA-D (mm)	6.0 ± 1.4	7.3 ± 1.3*	8.6 ± 1.7***	6.6 ± 1.7	7.3 ± 1.4†	8.6 ± 1.9†,††	6.3 ± 1.6	7.3 ± 1.4‡	8.2 ± 1.8‡,‡‡
TAP-D (mm)	9.5 ± 1.2	10.5 ± 1.0*	11.2 ± 1.0***	10.0 ± 1.5	10.4 ± 1.0	11.2 ± 1.1†,††	9.9 ± 1.3	10.4 ± 1.1‡	10.9 ± 1.1‡,‡‡
TAFS (%)	24.3 ± 10.1	21.1 ± 8.7	19.8 ± 7.0	26.1 ± 9.6	20.6 ± 8.5†	19.4 ± 8.0†	24.3 ± 10.8	21.4 ± 8.6	19.1 ± 7.4‡
TAFAC (%)	29.4 ± 12.3	26.5 ± 9.9	23.2 ± 10.5	32.5 ± 11.9	25.6 ± 10.1†	22.3 ± 9.0†	31.2 ± 11.8	25.9 ± 10.2‡	24.1 ± 10.0‡

$V_{max}$ , maximum end-systolic right atrial volume;  $V_{preA}$ , early diastolic pre-atrial contraction right atrial volume;  $V_{min}$ , minimum end-diastolic right atrial volume; TASV, total atrial stroke volume; TAEF, total (right) atrial emptying fraction; PASV, passive (right) atrial stroke volume; PAEF, passive (right) atrial emptying fraction; AASV, active (right) atrial stroke volume; AAEF, active (right) atrial emptying fraction; TAD, tricuspid annular diameter; TAA, tricuspid annular area; TAP, tricuspid annular perimeter; TAFS, tricuspid annular fractional shortening; TAFAC, tricuspid annular fractional area change; S, end-systolic; D, end-diastolic.

\* $p < 0.05$  vs.  $V_{max} \leq 33.8 \text{ ml}$ .  
 \*\* $p < 0.05$  vs.  $33.8 \text{ ml} < V_{max} < 64.0 \text{ ml}$ .  
 † $p < 0.05$  vs.  $V_{preA} \leq 24.8 \text{ ml}$ .  
 †† $p < 0.05$  vs.  $24.8 \text{ ml} < V_{preA} < 46.8 \text{ ml}$ .  
 ‡ $p < 0.05$  vs.  $V_{min} \leq 18.1 \text{ ml}$ .  
 ‡‡ $p < 0.05$  vs.  $18.1 \text{ ml} < V_{min} < 37.5 \text{ ml}$ .

TABLE 4 Right atrial volumes and tricuspid annular parameters in different end-systolic tricuspid annular groups.

	$TAD-S \leq 1.5 \text{ cm}$ (n = 16)	$1.5 \text{ cm} < TAD-S < 2.1 \text{ cm}$ (n = 102)	$2.1 \text{ cm} \leq TAD-S$ (n = 26)	$TAA-S \leq 4.0 \text{ cm}^2$ (n = 24)	$4.0 \text{ cm} < TAA-S < 6.8 \text{ cm}^2$ (n = 103)	$6.8 \text{ cm}^2 \leq TAA-S$ (n = 17)	$TAP-S \leq 7.9 \text{ cm}$ (n = 24)	$7.9 \text{ cm} < TAP-S < 10.1 \text{ cm}$ (n = 102)	$10.1 \text{ cm} \leq TAP-S$ (n = 18)
$V_{max}$ (ml)	35.6 ± 10.4	49.5 ± 14.4*	54.9 ± 15.6*	35.3 ± 9.8	50.0 ± 13.3†	61.3 ± 18.4†,††	36.7 ± 10.5	50.0 ± 13.7‡	58.6 ± 18.6‡,‡‡
$V_{preA}$ (ml)	27.0 ± 9.6	35.8 ± 10.1*	41.2 ± 11.9***	25.1 ± 6.9	36.5 ± 8.7†	46.2 ± 15.4†,††	27.6 ± 8.1	36.3 ± 9.4‡	43.4 ± 15.5‡,‡‡
$V_{min}$ (ml)	21.3 ± 9.6	27.5 ± 9.0*	32.8 ± 9.8***	19.1 ± 6.6	28.5 ± 8.4†	36.0 ± 11.7†,††	20.7 ± 7.5	28.4 ± 8.9‡	34.0 ± 11.4‡,‡‡
TASV (ml)	14.3 ± 6.4	22.0 ± 9.9*	22.1 ± 10.6*	16.2 ± 9.1	21.5 ± 9.5†	25.3 ± 11.7†	16.0 ± 8.9	21.7 ± 9.7‡	24.6 ± 10.9‡
TAEF (%)	40.9 ± 15.2	48.7 ± 11.9	39.0 ± 13.1	44.7 ± 15.1	42.3 ± 11.9	40.4 ± 13.1	42.7 ± 14.7	42.7 ± 12.4	41.2 ± 11.4
PASV (ml)	8.6 ± 6.1	13.7 ± 8.2*	13.7 ± 9.1*	10.2 ± 8.2	13.5 ± 7.9	15.1 ± 10.4	9.0 ± 7.4	13.7 ± 8.1‡	15.1 ± 9.5‡
PAEF (%)	23.9 ± 15.5	26.6 ± 10.9	23.8 ± 12.3	27.1 ± 15.9	25.7 ± 10.2	24.2 ± 14.0	23.5 ± 15.2	26.4 ± 10.6	25.6 ± 12.9
AASV (ml)	5.7 ± 2.3	8.3 ± 4.7*	8.3 ± 5.8	6.0 ± 3.4	8.1 ± 4.6†	10.2 ± 6.2†	6.9 ± 3.7	8.0 ± 4.6	9.4 ± 6.4
AAEF (%)	22.7 ± 10.6	23.3 ± 11.6	19.8 ± 11.9	24.3 ± 11.2	22.3 ± 12.0	21.5 ± 9.4	25.5 ± 10.3	22.2 ± 12.1	20.8 ± 10.1
TAD-S (mm)	1.4 ± 0.1	1.8 ± 0.1*	2.3 ± 0.2***	1.6 ± 0.2	1.8 ± 0.2†	2.2 ± 0.3†,††	1.7 ± 0.2	1.8 ± 0.2‡	2.2 ± 0.4‡,‡‡
TAA-S (mm)	4.0 ± 0.9	5.2 ± 1.2*	6.8 ± 1.6***	3.5 ± 0.4	5.4 ± 0.8†	8.1 ± 1.3†,††	3.7 ± 0.5	5.3 ± 0.9‡	7.8 ± 1.4‡,‡‡
TAP-S (mm)	8.2 ± 0.9	9.0 ± 1.0*	9.8 ± 1.1***	7.6 ± 0.6	9.1 ± 0.7†	10.8 ± 0.9†,††	7.4 ± 0.4	9.1 ± 0.6‡	11.0 ± 0.7‡,‡‡
TAD-D (mm)	2.1 ± 0.3	2.3 ± 0.2*	2.7 ± 0.3***	2.1 ± 0.2	2.4 ± 0.2†	2.7 ± 0.4†,††	2.1 ± 0.3	2.4 ± 0.3‡	2.6 ± 0.4‡,‡‡
TAA-D (mm)	5.7 ± 1.1	7.1 ± 1.3*	9.0 ± 1.6***	5.5 ± 1.0	7.3 ± 1.2†	9.7 ± 1.4†,††	5.7 ± 1.1	7.3 ± 1.2‡	9.6 ± 1.4‡,‡‡
TAP-D (mm)	9.4 ± 0.9	10.4 ± 1.1*	11.3 ± 1.0***	9.1 ± 0.8	10.5 ± 0.9†	12.0 ± 0.8†,††	9.2 ± 0.9	10.5 ± 0.9‡	12.0 ± 0.7‡,‡‡
TAFS (%)	31.3 ± 10.5	21.1 ± 8.2*	17.2 ± 5.1***	23.3 ± 9.4	21.6 ± 8.7	17.8 ± 7.8	21.8 ± 8.8	21.9 ± 8.9	18.3 ± 3.5
TAFAC (%)	30.2 ± 12.3	27.1 ± 12.6	24.4 ± 10.4	34.4 ± 10.3	26.1 ± 9.9†	17.1 ± 6.3†,††	33.4 ± 10.4	26.1 ± 10.3‡	18.8 ± 5.6‡,‡‡

$V_{max}$ , maximum end-systolic right atrial volume;  $V_{preA}$ , early diastolic pre-atrial contraction right atrial volume;  $V_{min}$ , minimum end-diastolic right atrial volume; TASV, total atrial stroke volume; TAEF, total (right) atrial emptying fraction; PASV, passive (right) atrial stroke volume; PAEF, passive (right) atrial emptying fraction; AASV, active (right) atrial stroke volume; AAEF, active (right) atrial emptying fraction; TAD, tricuspid annular diameter; TAA, tricuspid annular area; TAP, tricuspid annular perimeter; TAFS, tricuspid annular fractional shortening; TAFAC, tricuspid annular fractional area change; S, end-systolic; D, end-diastolic.

\* $p < 0.05$  vs.  $TAD-S \leq 1.5 \text{ cm}$ .  
 \*\* $p < 0.05$  vs.  $1.5 \text{ cm} < TAD-S < 2.1 \text{ cm}$ .  
 † $p < 0.05$  vs.  $TAA-S \leq 4.0 \text{ cm}^2$ .  
 †† $p < 0.05$  vs.  $4.0 \text{ cm} < TAA-S < 6.8 \text{ cm}^2$ .  
 ‡ $p < 0.05$  vs.  $TAP-S \leq 7.9 \text{ cm}$ .  
 ‡‡ $p < 0.05$  vs.  $7.9 \text{ cm} < TAP-S < 10.1 \text{ cm}$ .

TABLE 5 Right atrial volumes and tricuspid annular parameters in different end-diastolic tricuspid annular groups.

	TAD-D ≤ 2.1 cm (n = 41)	2.1 cm < TAD-D < 2.7 cm (n = 80)	2.7 cm ≤ TAD-D (n = 23)	TAA-D ≤ 5.7 cm <sup>2</sup> (n = 22)	5.7 cm < TAA-D < 8.9 cm <sup>2</sup> (n = 97)	8.9 cm <sup>2</sup> ≤ TAA-D (n = 25)	TAP-D ≤ 9.3 cm (n = 25)	9.3 cm < TAP-D < 11.7 cm (n = 95)	11.7 cm ≤ TAP-D (n = 24)
V <sub>max</sub> (ml)	43.4 ± 12.6	49.7 ± 15.6*	55.8 ± 14.7*	36.4 ± 9.5	48.8 ± 13.7 <sup>†</sup>	59.8 ± 16.5 <sup>†,††</sup>	36.3 ± 9.2	49.9 ± 13.6 <sup>‡</sup>	57.7 ± 17.5 <sup>‡,‡‡</sup>
V <sub>preA</sub> (ml)	31.9 ± 9.2	36.4 ± 10.6*	40.6 ± 13.1*	27.2 ± 7.8	35.9 ± 9.5 <sup>†</sup>	42.9 ± 13.5 <sup>†,††</sup>	27.8 ± 7.0	36.5 ± 10.0 <sup>‡</sup>	41.5 ± 13.4 <sup>‡,‡‡</sup>
V <sub>min</sub> (ml)	24.4 ± 9.0	28.3 ± 9.4*	31.9 ± 10.5*	20.5 ± 6.7	27.9 ± 9.0 <sup>†</sup>	33.7 ± 10.6 <sup>†,††</sup>	21.5 ± 6.8	28.1 ± 8.9 <sup>‡</sup>	32.8 ± 11.7 <sup>‡,‡‡</sup>
TASV (ml)	19.0 ± 9.8	21.4 ± 10.0	23.8 ± 9.9	15.9 ± 8.2	21.0 ± 9.7 <sup>†</sup>	26.2 ± 10.2 <sup>†,††</sup>	14.8 ± 7.8	21.8 ± 9.4 <sup>‡</sup>	24.9 ± 11.2 <sup>‡</sup>
TAEF (%)	43.1 ± 15.1	42.2 ± 11.0	42.3 ± 13.4	42.6 ± 14.2	42.3 ± 12.7	42.2 ± 11.0	40.0 ± 13.3	43.1 ± 12.4	42.6 ± 12.5
PASV (ml)	11.5 ± 7.2	13.3 ± 8.6	15.2 ± 8.9	9.2 ± 7.2	13.0 ± 8.0 <sup>†</sup>	16.9 ± 9.0 <sup>†,††</sup>	8.6 ± 6.4	13.4 ± 7.8 <sup>‡</sup>	16.2 ± 10.1 <sup>‡</sup>
PAEF (%)	25.6 ± 12.3	25.5 ± 11.2	27.1 ± 13.0	24.2 ± 14.8	25.5 ± 11.2	28.1 ± 11.0	22.6 ± 12.5	26.2 ± 11.2	27.2 ± 12.6
AASV (ml)	7.5 ± 4.9	8.0 ± 4.5	8.6 ± 5.6	6.7 ± 4.2	8.0 ± 4.5	9.2 ± 5.9	6.2 ± 4.8	8.3 ± 4.6 <sup>‡</sup>	8.7 ± 5.0
AAEF (%)	24.0 ± 13.9	22.2 ± 10.6	21.2 ± 10.4	24.2 ± 11.5	22.6 ± 11.9	21.0 ± 10.6	22.1 ± 13.7	23.1 ± 11.3	21.3 ± 10.3
TAD-S (mm)	1.6 ± 0.1	1.8 ± 0.2*	2.2 ± 0.3***	1.6 ± 0.1	1.8 ± 0.2 <sup>†</sup>	2.2 ± 0.3 <sup>†,††</sup>	1.6 ± 0.2	1.8 ± 0.3 <sup>‡</sup>	2.0 ± 0.3 <sup>‡,‡‡</sup>
TAA-S (mm)	4.4 ± 1.0	5.4 ± 1.1*	6.9 ± 1.7***	3.8 ± 0.5	5.3 ± 0.9 <sup>†</sup>	7.3 ± 1.6 <sup>†,††</sup>	3.9 ± 0.6	5.4 ± 1.1 <sup>‡</sup>	6.8 ± 1.7 <sup>‡,‡‡</sup>
TAP-S (mm)	8.2 ± 0.8	9.2 ± 1.0*	10.0 ± 1.1***	7.7 ± 0.7	9.0 ± 0.8 <sup>†</sup>	10.3 ± 1.1 <sup>†,††</sup>	7.9 ± 0.8	9.1 ± 0.9 <sup>‡</sup>	10.1 ± 1.1 <sup>‡,‡‡</sup>
TAD-D (mm)	2.0 ± 0.1	2.4 ± 0.1*	2.8 ± 0.2***	2.0 ± 0.2	2.3 ± 0.2 <sup>†</sup>	2.7 ± 0.3 <sup>†,††</sup>	2.1 ± 0.2	2.4 ± 0.3 <sup>‡</sup>	2.5 ± 0.4 <sup>‡,‡‡</sup>
TAA-D (mm)	6.0 ± 1.1	7.4 ± 1.2*	9.2 ± 1.4***	5.0 ± 0.5	7.2 ± 0.8 <sup>†</sup>	9.8 ± 1.1 <sup>†,††</sup>	5.3 ± 0.7	7.3 ± 1.0 <sup>‡</sup>	9.5 ± 1.4 <sup>‡,‡‡</sup>
TAP-D (mm)	9.8 ± 1.1	10.5 ± 1.0*	11.5 ± 1.0***	8.8 ± 0.6	10.4 ± 0.8 <sup>†</sup>	12.0 ± 0.6 <sup>†,††</sup>	8.8 ± 0.5	10.4 ± 0.7 <sup>‡</sup>	12.2 ± 0.4 <sup>‡,‡‡</sup>
TAFS (%)	18.0 ± 7.3	22.9 ± 9.4*	22.5 ± 7.6*	21.6 ± 7.1	21.8 ± 9.5	19.8 ± 7.1	22.8 ± 7.3	21.1 ± 9.4	21.3 ± 7.7
TAFAC (%)	26.9 ± 10.6	26.5 ± 10.7	25.5 ± 10.4	24.8 ± 9.8	26.9 ± 10.8	26.3 ± 10.5	26.5 ± 9.9	25.6 ± 10.8	29.5 ± 10.4

V<sub>max</sub>, maximum end-systolic right atrial volume; V<sub>preA</sub>, early diastolic pre-atrial contraction right atrial volume; V<sub>min</sub>, minimum end-diastolic right atrial volume; TASV, total atrial stroke volume; TAEF, total (right) atrial emptying fraction; PASV, passive (right) atrial stroke volume; PAEF, passive (right) atrial emptying fraction; AASV, active (right) atrial stroke volume; AAEF, active (right) atrial emptying fraction; TAD, tricuspid annular diameter; TAA, tricuspid annular area; TAP, tricuspid annular perimeter; TAFS, tricuspid annular fractional shortening; TAFAC, tricuspid annular fractional area change; S, end-systolic; D, end-diastolic.

\*p < 0.05 vs. TAD-D ≤ 2.1 cm.  
 \*\*p < 0.05 vs. 2.1 cm < TAD-D < 2.7 cm.  
 †p < 0.05 vs. TAA-D ≤ 5.7 cm<sup>2</sup>.  
 ††p < 0.05 vs. 5.7 cm < TAA-D < 8.9 cm<sup>2</sup>.  
 ‡p < 0.05 vs. TAP-D ≤ 9.3 cm.  
 ‡‡p < 0.05 vs. 9.3 cm < TAP-D < 11.7 cm.

systole, it closes to prevent backflow or regurgitation from the RV into the RA. The normal TA is a dynamic structure with a saddle-shape like MA, its dilation is accompanied with a more circular and planar shape (16, 17). Tricuspid regurgitation is organic only in 10–15% of cases (18), most of the cases show functional regurgitation (FTR) due to distorted RV, subvalvular apparatus, or TA, with structurally normal tricuspid leaflets (19, 20). FTR is mostly due to LV dysfunction, aortic or mitral valve disease or pulmonary vascular or interstitial disorders and is accompanied

with consequent pulmonary hypertension (PH). If FTR is secondary to TA dilation and leaflet tethering and associated to RV dilation and/or dysfunction, it has been called as “classical” or ventricular form of FTR for a long time. In case of absent PH or left heart disorders, FTR was called as idiopathic tricuspid regurgitation previously, which is related to age and atrial fibrillation (AF) (19, 20). Recently, a new distinct entity has been created called as atrial FTR, which can be found in AF patients, in which RA enlargement and dysfunction result in TA dilation,

TABLE 6 Intra- and interobserver variability for three-dimensional speckle-tracking echocardiography-derived tricuspid annular dimensions and right atrial volumes.

	Intraobserver agreement		Interobserver agreement	
	Mean ± 2SD difference in values obtained by 2 measurements of the same observer	ICC between measurements of the same observer	Mean ± 2SD difference in values obtained by 2 observers	ICC between independent measurements of 2 observers
End-diastolic TAD	0.02 ± 0.21 cm	0.96 (p < 0.0001)	0.03 ± 0.15 cm	0.96 (p < 0.0001)
End-diastolic TAA	−0.04 ± 1.14 cm <sup>2</sup>	0.95 (p < 0.0001)	0.02 ± 0.56 cm <sup>2</sup>	0.96 (p < 0.0001)
End-diastolic TAP	−0.03 ± 0.71 cm	0.95 (p < 0.0001)	−0.11 ± 0.58 cm	0.96 (p < 0.0001)
End-systolic TAD	−0.03 ± 0.32 cm	0.96 (p < 0.0001)	0.02 ± 0.44 cm	0.96 (p < 0.0001)
End-systolic TAA	−0.04 ± 0.31 cm <sup>2</sup>	0.95 (p < 0.0001)	−0.05 ± 0.65 cm <sup>2</sup>	0.97 (p < 0.0001)
End-systolic TAP	0.07 ± 0.55 cm	0.96 (p < 0.0001)	0.04 ± 0.59 cm	0.97 (p < 0.0001)
V <sub>max</sub>	1.2 ± 6.3 ml	0.96 (p < 0.0001)	1.0 ± 5.2 ml	0.95 (p < 0.0001)
V <sub>preA</sub>	−1.5 ± 8.6 ml	0.87 (p < 0.0001)	−1.5 ± 8.3 ml	0.90 (p < 0.0001)
V <sub>min</sub>	0.8 ± 5.1 ml	0.94 (p < 0.0001)	0.9 ± 4.6 ml	0.94 (p < 0.0001)

ICC, interclass correlation coefficient; TAD, tricuspid annular diameter; TAA, tricuspid annular area; TAP, tricuspid annular perimeter; SD, standard deviation; V<sub>max</sub>, maximum end-systolic right atrial volume; V<sub>preA</sub>, early diastolic pre-atrial contraction right atrial volume; V<sub>min</sub>, minimum end-diastolic right atrial volume.

leaflet malcoaptation and loss of TA sphincter-like function (21). Therefore, RA rather than RV dilation is more important to determine TA dilation and development of FTR in such cases (5). Similarly, following heart transplantation, overall RA diameter and native recipient RA diameter were found to be a risk factor for TA distension, which is reported to be a causative factor for the most common type of TV dysfunction (22).

Routine non-invasive TV assessment is based on 2D Doppler echocardiography, but results with 3D echocardiography are also available (23). 3DSTE has been demonstrated to be capable not only of performing RA chamber quantifications (14), but for determination of atrioventricular annular dimensions and its sphincter-like functional properties at the same time using the same 3D acquired datasets from the transthoracic window (15). Age- and gender-dependency and normal reference values for 3DSTE-derived RA and TA assessments were also determined with considerable intra- and interobserver agreements (14, 15). Therefore, 3DSTE seems to be an optimal option for simultaneous assessment of TA and RA for (patho)physiologic studies. According to present findings, although feasibility of simultaneous assessment of 3DSTE-derived RA volumes and TA dimensions proved to be limited, however, reproducibility was found to be acceptable in those cases where the measurements were feasible.

There can be a question whether associations between RA size and TA dimensions exist before FTR develops in healthy adults in sinus rhythm. It is known that with increasing left atrial volumes, mitral annulus dilated and became functionally impaired under healthy circumstances (24). The present study serves as an analogy for this by examining what happens in the right side of the heart under similar conditions. Results show similar findings demonstrating strong associations in case of dilation of TA in the presence of higher RA volumes. Moreover, dilation of TA and enlargement of RA predicted each other, as well. It is more important in the context of recent findings from the MAGYAR-Healthy Study, where strong associations between RA radial strains and end-diastolic TA area could also be detected in healthy subjects without FTR (9). However, further clinical studies are warranted to confirm our findings in a larger population or in different pathologic states and to demonstrate their possible clinical role in patient management. Moreover, long-term follow-up could confirm predictive role of TA/RA dilation on the development of AF and/or FTR.

## Limitations

Several important limitations have arisen during assessments:

- 2D echocardiography still allows TA assessment with a better image quality as compared to 3DSTE.
- The results would have been much more convincing if the measurement results had been validated against those measured with the Tomtekt software. This topic could even be the subject of a subsequent study.
- Although TA has a special 3D saddle-shape, only its 2D-projected image was determined.
- The study did not aim to compare 2D echocardiography vs. 3DSTE in the assessment of TA.
- Speckle-tracking analysis of TA functionality was not purposed, as well.
- FTR was excluded by visual assessment, more advanced quantification method was not applied during evaluations.

## Conclusions

3DSTE is suitable for non-invasive assessment of TA dimensions and RA volumes at the same time using the same 3D echocardiographic dataset. Significant associations between TA size and RA volumes exist in healthy circumstances. Strong associations in case of dilation of TA in the presence of higher RA volumes could partly explain FTR later developing in subjects in sinus rhythm.

## Data availability statement

The datasets presented in this article are not readily available due to local restrictions. Requests to access the datasets should be directed to nemes.attila@med.u-szeged.hu.

## Ethics statement

The study was conducted in accordance with the Declaration of Helsinki (as revised in 2013). The study was approved by the Institutional and Regional Human Biomedical Research Committee of University of Szeged, Hungary (No.: 71/2011 and updated versions) and informed consent was given by all subjects.

## Author contributions

AN—original idea, writing manuscript. ÁK—data collection, measurements. GR—data collection, measurements. ZR—writing manuscript. AA—writing manuscript. NA—writing manuscript, control. CL—writing manuscript, control. All authors contributed to the article and approved the submitted version.

## Conflict of interest

The authors declare that the research was conducted in the absence of any commercial or financial relationships that could be construed as a potential conflict of interest.



## Publisher's note

All claims expressed in this article are solely those of the authors and do not necessarily represent those of their affiliated

organizations, or those of the publisher, the editors and the reviewers. Any product that may be evaluated in this article, or claim that may be made by its manufacturer, is not guaranteed or endorsed by the publisher.

## References

- Lang RM, Badano LP, Mor-Avi V, Afilalo J, Armstrong A, Ernande L, et al. Recommendations for cardiac chamber quantification by echocardiography in adults: an update from the American society of echocardiography and the European association of cardiovascular imaging. *Eur Heart J Cardiovasc Imaging*. (2015) 16:233–70. doi: 10.1093/ehjci/jev014
- Rudski LG, Lai WW, Afilalo J, Hua L, Handschumacher MD, Chandresakaran K, et al. Guidelines for the echocardiographic assessment of the right heart in adults: a report from the American Society of Echocardiography endorsed by the European Association of Echocardiography, a registered branch of the European Society of Cardiology, and the Canadian Society of Echocardiography. *J Am Soc Echocardiogr*. (2010) 23:685–713. doi: 10.1016/j.echo.2010.05.010
- Muraru D, Hahn RT, Soliman OI, Faetra FF, Basso C, Badano LP. 3-Dimensional echocardiography in imaging the tricuspid valve. *JACC Cardiovasc Imaging*. (2019) 12:500–15. doi: 10.1016/j.jcmg.2018.10.035
- Tadic M. The right atrium, a forgotten cardiac chamber: an updated review of multimodality imaging. *J Clin Ultrasound*. (2015) 43:335–45. doi: 10.1002/jcu.22261
- Guta AC, Badano LP, Tomaselli M, Mihalcea D, Bartos D, Parati G, et al. The pathophysiological link between right atrial remodeling and functional tricuspid regurgitation in patients with atrial fibrillation: a three-dimensional echocardiography study. *J Am Soc Echocardiogr*. (2021) 34:585–594.e1. doi: 10.1016/j.echo.2021.01.004
- Muraru D, Addetia K, Guta AC, Ochoa-Jimenez R, Genovese D, Veronesi F, et al. Right atrial volume is a major determinant of tricuspid annulus area in functional tricuspid regurgitation: a three-dimensional echocardiography study. *Eur Heart J Cardiovasc Imaging*. (2021) 22:660–9. doi: 10.1093/ehjci/jeaa286
- Florescu DR, Muraru D, Florescu C, Volpato V, Caravita S, Perger E, et al. Right heart chambers geometry and function in patients with the atrial and the ventricular phenotypes of functional tricuspid regurgitation. *Eur Heart J Cardiovasc Imaging*. (2022) 23:930–40. doi: 10.1093/ehjci/jeab211
- Muraru D, Gavazzoni M, Heilbron F, Mihalcea DJ, Guta AC, Radu N, et al. Reference ranges of tricuspid annulus geometry in healthy adults using a dedicated three-dimensional echocardiography software package. *Front Cardiovasc Med*. (2022) 9:1011931. doi: 10.3389/fcvm.2022.1011931
- Nemes A, Kormányos Á, Ruzsa Z, Achim A, Ambrus N, Lengyel C. Three-dimensional speckle-tracking echocardiography-derived tricuspid annular dimensions and right atrial strains in healthy adults—is there a relationship? (insights from the MAGYAR-Healthy Study). *J Clin Med*. (2023) 12:4240. doi: 10.3390/jcm12134240
- Urbano-Moral JA, Patel AR, Maron MS, Arias-Godinez JA, Pandian NG. Three-dimensional speckle-tracking echocardiography: methodological aspects and clinical potential. *Echocardiography*. (2012) 29:997–1010. doi: 10.1111/j.1540-8175.2012.01773.x
- Ammar KA, Paterick TE, Khandheria BK, Jan MF, Kramer C, Umland MM, et al. Myocardial mechanics: understanding and applying three-dimensional speckle tracking echocardiography in clinical practice. *Echocardiography*. (2012) 29:861–72. doi: 10.1111/j.1540-8175.2012.01712.x
- Muraru D, Niero A, Rodriguez-Zanella H, Cherata D, Badano L. Three-dimensional speckle-tracking echocardiography: benefits and limitations of integrating myocardial mechanics with three-dimensional imaging. *Cardiovasc Diagn Ther*. (2018) 8:101–17. doi: 10.21037/cdt.2017.06.01
- Lancellotti P, Tribouilloy C, Hagendorff A, Popescu BA, Edvardsen T, Pierard LA, et al. Recommendations for the echocardiographic assessment of native valvular regurgitation: an executive summary from the European Association of Cardiovascular Imaging. *Eur Heart J Cardiovasc Imaging*. (2013) 14:611–44. doi: 10.1093/ehjci/jet105
- Nemes A, Kormányos Á, Domsik P, Kalapos A, Ambrus N, Lengyel C. Normal reference values of three-dimensional speckle-tracking echocardiography-derived right atrial volumes and volume-based functional properties in healthy adults (Insights from the MAGYAR-Healthy Study). *J Clin Ultrasound*. (2020) 48:263–8. doi: 10.1002/jcu.22795
- Nemes A, Kormányos Á, Rác G, Ruzsa Z, Ambrus N, Lengyel C. Normal reference values of tricuspid annular dimensions and functional properties in healthy adults using three-dimensional speckle-tracking echocardiography (insights from the MAGYAR-Healthy Study). *Quant Imaging Med Surg*. (2023) 13:121–32. doi: 10.21037/qims-22-88
- Ton-Nu TT, Levine RA, Handschumacher MD, Dorer DJ, Yosefy C, Fan D, et al. Geometric determinants of functional tricuspid regurgitation: insights from 3-dimensional echocardiography. *Circulation*. (2006) 114:143–9. doi: 10.1161/CIRCULATIONAHA.106.611889
- Addetia K, Muraru D, Veronesi F, Jenéi C, Cavalli G, Besser SA, et al. 3-dimensional echocardiographic analysis of the tricuspid annulus provides new insights into tricuspid valve geometry and dynamics. *JACC Cardiovasc Imaging*. (2019) 12:401–12. doi: 10.1016/j.jcmg.2017.08.022
- Muraru D, Addetia K, Jarjour F, Lang RM, Badano LP. Organic tricuspid regurgitation. In: Badano LP, Lang RM, Muraru D, editors. *Textbook of three-dimensional echocardiography*. Cham, Switzerland: Springer (2019). p. 271–83
- Gual-Capllonch F, Cediel G, Ferrer E, Teis A, Juncà G, Vallejo N, et al. Sex-related differences in the mechanism of functional tricuspid regurgitation. *Heart Lung Circ*. (2021) 30:e16–22. doi: 10.1016/j.hlc.2020.06.018
- Badano LP, Muraru D, Enriquez-Sarano M. Assessment of functional tricuspid regurgitation. *Eur Heart J*. (2013) 34:1875–85. doi: 10.1093/eurheartj/ehs474
- Florescu DR, Muraru D, Volpato V, Gavazzoni M, Caravita S, Tomaselli M, et al. Atrial functional tricuspid regurgitation as a distinct pathophysiological and clinical entity: no idiopathic tricuspid regurgitation anymore. *J Clin Med*. (2022) 11:382. doi: 10.3390/jcm11020382
- Urbanowicz T, Michalak M, Kociemba A, Straburzyńska-Migaj E, Katarzyński S, Grajek S, et al. Predictors of tricuspid valve annulus dilation in a heart recipient population. *Transplant Proc*. (2016) 48:1742–5. doi: 10.1016/j.transproceed.2016.01.093
- Anwar AM, Geleijnse ML, Soliman OII, McGhie JS, Frowijn R, Nemes A, et al. Assessment of normal tricuspid valve anatomy in adults by real-time three-dimensional echocardiography. *Int J Cardiovasc Imaging*. (2007) 23:717–24. doi: 10.1007/s10554-007-9210-3
- Nemes A, Kormányos Á, Ambrus N, Lengyel C. Associations between mitral annular and left atrial volume changes in healthy adults—Detailed analysis from the three-dimensional speckle-tracking echocardiographic MAGYAR-Healthy Study. *Rev Cardiovasc Med*. (2022) 23:194. doi: 10.31083/j.rcm2306194